Nozzle," UTC 2296-FR, March 1969, United Technology Center, Sunnyvale, Calif.

[94] Schlichting, H., *Boundary Layer Theory,* McGraw-Hill, New York, March 1958, pp. 97–98.

[95] McAdams, W., *Heat Transmission,* 3rd ed., McGraw-Hill, New York, 1954, pp. 265–266.

[96] Emmons, H. W., *Fundamentals of Gas Dynamics, High Speed Aerodynamics and Jet Propulsion,* Vol. 3, Princeton Univ. Press, Princeton, N.J., 1958, p. 725.

[97] Wiederkehr, R. R. V., "A General Method for Calculating the Specific Impulse of Propellant Systems," AR-1S-60, (N-84819), June 1960, Dow Chemical Co., Midland, Mich.

[98] Unger, E. W., "Heat Transfer to a Solid Propellant Rocket Motor Nozzle," Preprint 2333-62, (IAA Abstract 62-10244), Jan. 1962, American Rocket Society.

[99] Elliott, D. G., Bartz, D. R., and Silver, S., "Calculation of Turbulent Boundary Layer Growth and Heat Transfer in Axi-Symmetric Nozzles," TR 32-387, (N63-14465), Feb. 1963, Jet Propulsion Lab.

[100] Kalt, S. and Badal, D. L., "Conical Rocket Nozzle Performance Under Flow-Separated Conditions," *Journal of Spacecraft and Rockets,* Vol. 2, No. 3, May-June 1965, pp. 447–449.

[101] Garrett, J. W., Simmons, M., and Gobbell, W. C., "Exit Nozzle Flow Separation as Influenced by Nozzle Geometry, Fuel-Oxidizer Ratio, and Pressure Level," AEDC-TR-67-122, (AD 816650), July 1967, Arnold Engineering Development Center, Arnold Air Force Station, Tenn.

[102] Sutton, G. P., *Rocket Propulsion Elements,* Wiley, New York, April 1964, pp. 37–83.

[103] Arena, M. and Spiegler, E., "Separated Flow in Overexpanded Nozzles at Low Pressure Ratios," *The Bulletin of the Research Council of Israel, Sec. C, Technology,* 11C, April 1962, pp. 45–55.

[104] Altman, D. et al., *Liquid-Propellant Rockets,* Princeton Aeronautical Paperbacks, Princeton Univ. Press, Princeton, N.J., 1960.

[105] Bloomer, H. E., Antl, R. J., and Renas, P. E., "Experimental Study of Effects of Geometric Variables on Performance of Conical Rocket-Engine Exhaust Nozzles," TN-D-846, June 1961, NASA.

[106] Roschke, F. J. and Massier, P. F., "Flow Separation in a Contour Nozzle," *ARS Journal,* Oct. 1962, pp. 1612–1613.

[107] Campbell, C. E. and Farley, J. M., "Performance of Several Conical Convergent-Divergent Rocket-Type Exhaust Nozzles," TN-D467, Sept. 1960, NASA.

[108] Lawrence, R. A. and Weynand, E. E., "Factors Affecting Flow Separation in Contoured Supersonic Nozzles," *AIAA Journal,* Vol. 6, No. 6, June 1968, pp. 1159–1160.

MARCH 1970 J. SPACECRAFT VOL. 7, NO. 3

Astrionics Selection and Operation on Interplanetary Missions

ELLIS F. HITT* AND FRED G. REA†
Battelle Memorial Institute, Columbus, Ohio

Selection of astrionics subsystems for automated spacecraft designed for interplanetary missions is accomplished using evaluation techniques which consider mission requirements, mission event schedules, and spacecraft design characteristics. These techniques provide a measure of astrionics system performance, aid in evaluation of competitive subsystems and in the preliminary design of conceptual subsystems, and are used in determination of the effectiveness of specific navigation updating and midcourse correction schedules. Using computer programs implementing these techniques, various astrionic systems were evaluated on alternate mission schedules for a Jupiter flyby mission. Results illustrate the usefulness of the techniques for selection of astrionics configurations, and evaluation of mission operation schedules which consider subsystem operation times, navigation updating with Kalman filtered measurements from Earth-based radars and onboard electro-optical sensors, and midcourse correction schedules.

Nomenclature

D_T, D_V = degrees of freedom of the target miss and midcourse ΔV covariances, respectively
P_{FA} = probability of mission failure attributable to the astrionics system
P_{FR} = probability of failure attributable to lack of astrionics reliability
P_{FT} = probability of excessive target miss
P_{FV} = probability of failure due to having insufficient midcourse fuel
Prob (ψ,D) = probability a vector's magnitude will exceed ψ times the square root of the trace of its covariance matrix
W_{AC} = weight of attitude control subsystem
W_{AH} = weight of astrionics hardware (inertial sensing unit, computer, communications, and electro-optical components)
W_{AT} = $W_{AC} + W_{AH} + W_{DV} + W_{ES}$
W_{DV} = weight of midcourse correction subsystem
W_{ES} = weight of electrical energy source
ΔV = midcourse correction velocity vector
$\psi(P,D)$ = inverse function of Prob (ψ,D)

Presented as Paper 69-882 at the AIAA Guidance, Control, and Flight Mechanics Conference, Princeton, N.J., August 18–20, 1969; submitted August 25, 1969; revision received November 3, 1969. This paper is based on work accomplished by Battelle Memorial Institute under Contract NAS 12-550 for the NASA, Electronics Research Center, Cambridge, Mass.

* Senior Systems Engineer, Systems and Electronics Department, Columbus Laboratories.

† Senior Systems Engineer, Systems and Electronics Department, Columbus Laboratories. Member AIAA.

Introduction

THE complexity and cost of astrionics for automated spacecraft and launch vehicles requires careful evaluation prior to committing major expenditure of funds for new programs. Techniques developed for evaluation of strapdown guidance systems[1] are extended to permit evaluation of aided inertial guidance systems and subsequently the complete astrionics. It is assumed that the principal astrionics subsystems are located above the last powered launch vehicle stage. This approach includes the weight of the astrionics in the final injected payload weight. Therefore, the astrionics can be considered to provide all navigation, guidance, and control functions for the launch vehicle and spacecraft (as is done for the mission under consideration), or for the launch

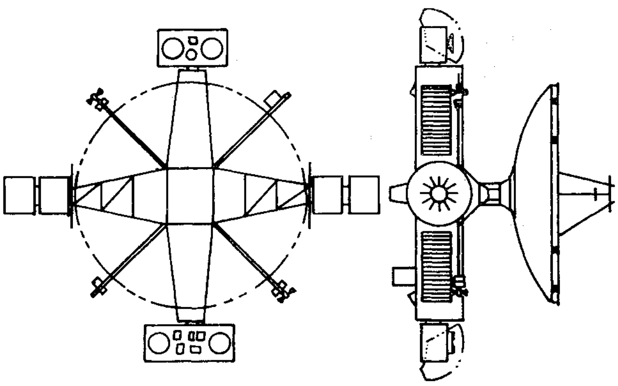

Fig. 1 Two views of nominal spacecraft for Jupiter flyby mission.

vehicle only if the spacecraft designers do not desire to make use of the capabilities of the principal subsystems.

A Jupiter flyby mission is considered, and it is assumed that the astrionics are an integral part of the spacecraft. The subsystems considered are:

1) The attitude control subsystem (ACS), which provides the required torques for stabilization and maneuvering of the spacecraft by 6 pairs of thruster nozzles driven with cold gas from a single tank. (Other mechanizations, such as reaction wheels plus jets or control moment gyroscopes, could be considered.)

2) The inertial sensing unit (ISU), which is strapdown since gimballed platforms considered in the work yielded less scientific payload weight on the Jupiter flyby mission than did strapdown.[2]

3) A centralized, general-purpose, digital computer, which provides 1) navigation, guidance, and control computations, 2) processing of data input and output to the communications subsystem, 3) control of all subsystem functions such as sequencing, and 4) data storage and processing.

4) The communications subsystem, which includes onboard antennas, transponder, command decoder, and multiplexer, and Earth-based tracking radars.

5) Electro-optical sensors (sun sensors and strapdown star trackers; horizon sensors and gimballed star trackers also were considered).

6) The electrical power source and distribution network.

The parameters used in the evaluation and selection of subsystem components are, in general: weight, power, mean-time-to-failure (MTTF) and Weibull coefficient, and performance, which depends upon the functions of the particular subsystems.

Evaluation Criteria

Effectiveness evaluation is based on a cost effectiveness approach with cost defined to be the total astrionics system weight and effectiveness defined to be the probability the astrionic system operates correctly. Using this cost or weight effectiveness model, several performance indices have been developed. These may be broken into two categories. The first category requires a specified effectiveness or probability and uses weight as the performance index, while the second category has a specified weight allowance for the astrionics and uses the ineffectiveness or probability of failure as the performance index. Evaluations discussed in this paper were made using the first category, i.e., with the probability the astrionics system operates correctly, 1-P_{FA}, specified as a mission constraint. The astrionics system weight, W_{AT}, is the performance index and is obtained by complete analysis of the astrionics, mission schedule, and spacecraft data.

The total astrionics weight is defined to be the sum of the weights of the subsystems shown in Fig. 1 and can be expressed by Eq. (1):

$$W_{AT} = W_{AH} + W_{ES} + W_{AC} + W_{DV} \tag{1}$$

The probability the astrionics system operates correctly may be expressed in terms of the probability of three chance events. These events are the failure of any astrionics subsystem due to lack of reliability, the failure of the midcourse correction(s) due to lack of sufficient midcourse fuel, and the failure to achieve the desired target accuracy. These probability relationships are expressed in Eq. (2):

$$1 - P_{FA} = (1 - P_{FR})(1 - P_{FV})(1 - P_{FT}) \tag{2}$$

The astrionics system parameters needed for evaluation of Eqs. (1) and (2) are obtained from detailed mathematical models of the astrionics systems and its operation on a specified interplanetary trajectory according to a detailed mission schedule. The astrionics hardware weight, W_{AH}, is simply the sum of the hardware weights of all the astrionics subsystem components being carried. The weight of the energy source, W_{ES}, is obtained from a simple model which includes a constant and coefficients relating weight to total energy and total peak power required. The weight of the attitude control subsystem, W_{AC}, is obtained from a detailed analysis of the attitude control requirements which are determined by the schedule requirements for spacecraft maneuvering to acquire the proper celestial bodies with the electro-optical sensors, midcourse correction orientation, and other schedule dependent attitude maneuvers. The weight of the midcourse system, W_{DV}, is determined from the total weight of the spacecraft, the specific impulse of the midcourse engine, the constant weight of nozzles and supporting electronics, a tankage factor, and the total midcourse engine ΔV capability requirements. The ΔV capability required must be calculated from the probability relationships of Eq. (2) and the probability distribution function of the midcourse correction ΔV. The probability of midcourse correction failure due to lack of sufficient fuel in terms of the other probabilities is shown in Eq. (3):

$$P_{FV} = 1 - \{(1 - P_{FA})/[(1 - P_{FR})(1 - P_{FT})]\} \tag{3}$$

The required midcourse correction capability is then found as shown in Equation (4):

$$\Delta V_c = R_V \psi(P_{FV}, D_V) \tag{4}$$

where the square root of the trace of the covariance of the midcourse ΔV, R_V, and the degrees of freedom of this covariance, D_V, are obtained from the error analysis. The function ψ shown in Eq. (4) is discussed in detail by Fischer and Rea.[3]

The probability of missing the target, P_{FT}, by more than the prescribed distance, $X_{\rm MISS}$, is treated in a similar manner. In this case, the square root of the trace of the covariance matrix of the target miss, R_T, and the degrees of freedom of target miss covariance, D_T, are known from the error analysis. The probability of target miss may then be found by Eqs. (5) or (6)

$$X_{\rm MISS}/R_T = \psi(P_{FT}, D_T) \tag{5}$$

or solving for P_{FT},

$$P_{FT} = \text{Prob } (X_{\rm MISS}/R_T, D_T) \tag{6}$$

where the function Prob is the inverse function of ψ.

In summary, for the results presented herein, the effectiveness evaluation is based on the total astrionics system weight. Reliability and other probabilistic effects are included by assuming sufficient midcourse fuel is carried to meet the required overall probability of astrionics system success. It should be noted that if any of the subprobabilities, such as the probability of failure due to lack of reliability or the probability of failure due to target miss, exceeds the allowed probability of astrionics failure, no amount of midcourse fuel will meet the requirements and the performance index is assumed to be undefined or saturated.

Error Analysis of Aided Inertial Navigation

A 9-element state vector is used to describe the system for error analysis. The 9 elements consist of: 3 position, 3 velocity, and 3 small angle attitude uncertainties in a rectangular coordinate system, oriented with one axis in the direction of the velocity vector, the second axis lies in the position-velocity plane, and the third completes the orthogonal triad. Three possible state vectors are considered at any moment in time on the mission. They are: $\mathbf{x}_a$, $\mathbf{x}_0$, and $\mathbf{x}_c$, the actual, nominal, and computed states of the vehicle, respectively.

For the purposes of error analysis, the following quantities are treated as normally distributed vectors with known covariances and zero means: $\mathbf{e} = \mathbf{x}_c - \mathbf{x}_a$, the error vector; $\mathbf{d} = \mathbf{x}_a - \mathbf{x}_0$, the deviation vector; $\mathbf{d}_c = \mathbf{x}_c - \mathbf{x}_0 = \mathbf{e} + \mathbf{d}$, the computed deviation of the vehicle.

The error vector, $\mathbf{e}$, represents the difference between the computed state and the actual state of the vehicle. An ideal measurement and update would set $\mathbf{e}$ equal to zero by making a step change in $\mathbf{x}_c$. The deviation vector $\mathbf{d}$ represents the difference between the actual state and the nominal state of the vehicle. Physical changes to the state of the system such as midcourse corrections, make step changes in $\mathbf{x}_a$ and thus change $\mathbf{d}$. The computed deviation vector, $\mathbf{d}_c$, represents the navigation system's information concerning the deviation of the spacecraft from the nominal. Updates and physical changes make step changes to $\mathbf{d}_c$.

Powered flight from the launch pad to a 100-naut-mile parking orbit and from the parking orbit to the escape hyperbola are analyzed assuming perfect closed-loop control of the launch vehicle using the astrionics system ISU and the digital computer for navigation, guidance, and control computations. The flight control subsystem is assumed to operate perfectly, so that the computed deviations, $\mathbf{d}_c$, are equal to zero and the errors are equal but opposite in algebraic sign to the deviations. Sensitivity matrices describing state errors at the end of the powered flight segment as a function of hardware error sources are generated using computer programs for either platform or strapdown error analysis. The error sources are assumed to be statistical biases (random ensembles constant in time) during the periods of powered flight.

Error propagation in a perfect 100-naut-mile parking orbit is analyzed by using a closed-form solution for the differential equation of error propagation. While in the parking orbit the spacecraft and astrionics are still attached to the booster. Thus, attitude control is assumed to be maintained by the booster torquers, with steering commands calculated by the astrionics digital computer utilizing outputs from the ISU.

The interplanetary trajectory and the associated state transition matrices were obtained by a modification to the Lewis n-body code.[4] Attitude control is analyzed as specified in the mission schedule and may be uncontrolled, stabilized by the gyros, or locked on celestial bodies observable by the electro-optical sensors. The error analysis implications of turning the various astrionics subsystems on and off during the flight, as specified in the schedule, are modeled. For example, if the ACS is not operative, complete uncertainty of the spacecraft attitude is assumed. The covariance of the attitude subset of the deviation vector $\mathbf{d}$ and the computed deviation $\mathbf{d}_c$ of the attitude subset, are equal to the covariance of a rectangular distribution from $-\pi$ to $+\pi$ rad.

Updates and Corrections

Measurement updates may be made by specifying in the schedule when the update is to occur and what measurement technique is to be used. The update is assumed to be performed with a Kalman filter which contains a perfect error model. Each potential method of updating is modeled to generate the appropriate measurement matrix and measurement covariance needed for the Kalman update. The following update techniques are available along with the indicated list of measured quantities: 1) ground based radar-range, range rate, azimuth, and elevation depending on the particular tracking radar used, and 2) sun sensors and star trackers—components of attitude normal to the line of sight.

All measurement errors are considered to be white-noise uncorrelated in time. Use of the filter thus can produce deceptively optimistic answers if updates using the same measurement subsystem are specified closer in time than the correlation time of the true sensor errors.

Midcourse corrections may be specified at any time in the mission after separation from the booster. The midcourse correction is assumed to be made at the specified time to minimize the computed deviation of a specified component or up to three components of the position or velocity vector at the target time. If less than three components are to be minimized at the target, the midcourse correction ΔV vector is not a unique function of the computed deviation vector. In this case, the correction with the minimum ΔV magnitude is assumed to be made. It should be noted that midcourse corrections are made as a function of the computed deviations, $\mathbf{d}_c$, at that point in the mission. If no updates have been made since the powered flight, the errors are equal and opposite to the deviations, and the computed deviations are zero. Thus, the midcourse correction will be zero. R_V and D_V are calculated. D_V is calculated by dividing R_V^2 by the sum of the square of the elements of the covariance matrix. Multiple midcourses are handled by taking the square root of the sum of the squares of the R_V of each correction and the sum of the degrees of freedom weighted by the R_V of each midcourse correction. Errors generated in making the midcourse correction are assumed to be due to two sources. The ISU accelerometers are assumed to be used to control the magnitude of the midcourse engine burn and the errors in the magnitude of the midcourse burn are calculated from the accelerometer error coefficients. The pointing errors in the midcourse correction are obtained by taking the cross product of the ΔV vector with the attitude subset of the error vector. Since both of these quantities are described as zero mean gaussian variables, an approximation must be used because the cross product will have a mean and higher moments.

Target Miss

Errors, deviations, and computed deviations are propagated from the last entry in the mission schedule to the time of nominal target arrival. At this point, the square root of the trace of the covariance matrix and the degrees of freedom of the covariance matrix of the target miss are obtained. Target miss may be defined to be any component of the state vector at the target or the radial miss distance from the nominal target point. For the cases discussed in this paper, the target requirement is assumed to be only the magnitude of the periapsis vector. Thus, only one component of position at the target point is of interest when considering target miss.

Mission Schedule

The detailed mission schedule must insure that proper use is made of a selected suite of astrionics subsystems, and it must include the times and other parameters necessary to define the following operations: 1) turning on or off any astrionics subsystem, 2) changes to the attitude-control-subsystem dead zone, 3) beginning the attitude maneuver necessary to orient the electro-optical sensors toward the nominal location of the required celestial bodies, 4) the end of the acquisition maneuver and the beginning of the search operation, 5) the end of the search operation, 6) ground based radar update with any specified radar, and 7) midcourse correction to minimize indicated component(s) of position or velocity at the target arrival.

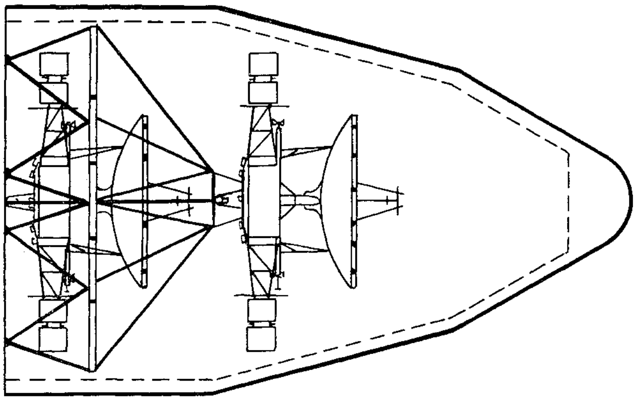

Fig. 2 Sketch of two nominal spacecraft, adapters, and shroud.

The effectiveness evaluation techniques previously discussed have been coded into a FORTRAN IV computer program for running on a Control Data 6400 computer. The following types of output are available from the program:

1) Level 1 evaluation: a 1-page report summarizing the astrionics subsystem parameters and the effectiveness evaluation calculations.

2) Level 2 evaluation: a 5- to 10-page printout of all mission operations and error analysis quantities as a function of time from the beginning of the mission to arrival at the target point.

3) Sensitivity analysis: (percent change in effectiveness per percent change in any data value) for mission, spacecraft, and astrionics data or selected subsets of data, to identify the subsystem parameters and mission values with the greatest impact on astrionics effectiveness.

4) Optimum system selection by successive substitution of candidate subsystems for evaluation. The substitution algorithm is similar to a steepest descent technique and has the potential for finding only local minima. However, multiple starting points minimize the probability that the system found is a local rather than a global optimum.

Mission schedule 1 used herein is shown in Table 1. Mission schedule 2 is identical to schedule 1 except that the sequence conducted from 400D0H30M0S to 400D1H2M0S was also conducted beginning at 200D0H30M0S. The times shown are times used for starting sequences of operations, and these events should not necessarily be interpreted as occuring simultaneously or, for a given time, in the sequence shown.

The conceptual 260(3.7)/SIVB/Centaur I/Kick launch vehicle was assumed to be suitable for the Jupiter flyby mission. A version of this vehicle has been studied by Battelle Columbus Laboratories, NASA Launch Vehicle Planning Project under Contract NASw-1146. The 260(3.7) first stage is a solid-propellant, single-engine stage.[5] The SIVB second stage is the current SIVB used by the Saturn family of launch vehicles. The Centaur I third stage is based on design evolution and concentrated development effort to employ hydrogen-fluorine propellants.[6] The "Kick" fourth stage is a small high-energy stage originally proposed for use with the SLV3C and the SLV3C/Centaur.[6] The powered flight trajectory for this launch vehicle was simulated to generate the data required for obtaining the strapdown system sensitivity matrix.

The vehicle was launched into a 100-naut-mile circular parking orbit. At 25 min into the mission (935 sec in the parking orbit), a Kalman filtered state update was made using the Ascension Island TPQ18 radar. After the state update, the vehicle continued in the parking orbit for 81.3 sec at which time the injection burn was started. The total action time of the three stages used for the injection burn was 941.5 sec. After completion of the injection burn, the spacecraft was separated from the launch vehicle and the attitude control system turned on at 42 min, 3 sec, as shown in Table 1.

Calculation of the ACS weight requires certain nominal values for the spacecraft parameters. The injected weight on the nominal trajectory being used in this study is 5410 lb.[1] A dual launch of a spacecraft similar to the one studied by General Dynamics[7] is quite feasible using the conceptual launch vehicle assumed for this study. Figure 1 depicts two views of the nominal spacecraft, and Fig. 2 depicts the two spacecraft in the shroud used by Battelle in the trajectory simulations. The adapter mating the upper spacecraft to the launch vehicle is shown. The various physical parameters used were based upon this scaled up version of the General Dynamics spacecraft design. The midcourse propulsion system was assumed to be a gas pressure-regulated monopropellant hydrazine unit using a Shell 405-type catalyst.[7] Guidance system electrical power was assumed to be supplied by a radioisotope thermoelectric generator onboard the spacecraft.

Results

An effectiveness evaluation of an astrionics system known as the reference system was performed. The reference system consists of three D4E accelerometers and three GG334A gyroscopes mounted on a strapdown ISU, which was designed by the program by evaluating several possible parts layouts and selecting a standard design from six alternative configurations. The excitation energy and power, total probability of failure, and total weight of the ISU are 109.5 w-hr, 43.5 w, 0.00063, and 33.46 lb, respectively, for mission schedule 1. The evaluation assumed the ISU is mounted on a variable thermal impedance, whose impedance may change by a ratio of 2:1. Heating power was calculated and added to the ISU excitation energy and excitation power to give the total energy, 176.7 w-hr, and total power, 141.4 w, for the ISU including the heaters.

The reference system includes a hypothetical computer known as the SRT computer utilizing a second-order, Runge-Kutta algorithm in the updating of the direction cosine matrix.[2] A strapdown star tracker, sun sensor, and a communications receiver complete the reference system. The

Table 1 Jupiter flyby mission schedule 1

Time[a]	Operation description
0*D* 0*H* 0*M* 0*S*	Start launch; turn on communication receiver
0*D* 0*H*25*M* 0*S*	Uptake with Ascension TPQ radar
0*D* 0*H*42*M* 3*S*	Turn on ACS
	Raise dead band to 20°
	Turn on star tracker and sun sensor
	Begin maneuvering
0*D* 0*H*57*M* 3*S*	Begin search
0*D* 0*H*58*M* 3*S*	End search
	Turn off ISU and computer
0*D*10*H* 0*M* 0*S*	Turn on computer and ISU
0*D*10*H*30*M* 0*S*	Drop dead band to 0.1°
	Update with any USBS-30
0*D*10*H*31*M* 0*S*	Make midcourse correction
	Raise dead band to 20°
	Turn off astrionics subsystems[b]
400*D* 0*H* 0*M* 0*S*	Turn on astrionics subsystems[b]
	Begin maneuvering
400*D* 0*H*30*M* 0*S*	Begin search
400*D* 0*H*31*M* 0*S*	End search
400*D* 1*H* 1*M* 0*S*	Drop dead band to 0.1°
	Update with any DSIF
400*D* 1*H* 2*M* 0*S*	Make midcourse correction
	Turn off astrionics subsystems[b]
410*D*10*H* 4*M* 2*S*	End of schedule

[a] Time in days (*D*), hours (*H*), minutes (*M*), and seconds (*S*) from liftoff.
[b] Star tracker, sun sensor, ACS, ISU, and computer.

Table 2 Summary of results

System	Schedule	$R_T \times 10^{-6}$, ft	R_V, fps	W_{DV}, lb	W_{AC}, lb	Performance index value, lb
Ref. 1[a]	1	1.54	14.985	28.515	21.21	343.460
Ref. 2[b]	1	5.49	14.984	28.514	21.21	343.459
Ref. 1[a]	2	0.153	14.945	28.571	21.40	343.700
Optimum[c]	1	1.90	7.428	24.377	21.21	331.448
Optimum[c]	2	0.255	7.386	24.392	21.40	331.645

	Gyros	Accelerometers	Computer	Sun sensor	Star tracker	Receiver
[a] Ref. 1	GG 334-A	D-4E	SRT	Adcole 1402	ITT Lunar orbiter	503
[b] Same as Ref. 1 with degraded radar						
[c] Optimum for schedule 1	18-IRIG	GG-177	SIGN III	Adcole 1402	ITT Lunar orbiter	503

system parameters of energy, power, probability of failure, and weight for these subsystems were found to be 33,971 w-hr, 106.5 w, 0.092, and 48.1 lb, respectively, for mission schedule 1.

The ACS parameters were calculated using results of the schedule evaluation and the sensors' fields of view. The various thrust sizing requirements were determined for the roll, yaw, and pitch axes. The worst case on each axis was taken as the design requirement yielding a thrust of 0.01 lb for the roll axis thrusters and 0.38 lb for the yaw and pitch axes thrusters. The large thrust requirements on the yaw and pitch axes were due to the need to steer the vehicle during the midcourse correction burn. Fuel consumption was calculated using these design thrusts. The total impulse (lb-sec) required for each axis was 4.34 (roll), 2.91 (yaw), and 0.45 (pitch). Searching dominated fuel consumption in roll and yaw, while deadband consumption dominated the pitch axis. From the total fuel consumption, the number of thruster firings, total impulse requirements, and attitude control subsystems fuel weights were then calculated. From these results, the total electrical energy and power, total probability of failure, and total weight are 108.5 w-hr, 10 w, 0.0028, and 21.22 lb, respectively for mission schedule 1.

The energy source weight is calculated as a function of the total power and total energy requirements. For the evaluations discussed in this paper, an RTG was assumed. The weight of this type of energy source is a function only of the total power requirement and the energy calculations are not used. The weight of the energy source was estimated to be 102 lb. An additional 110 lb is included to account for electrical distribution wiring.

The midcourse correction subsystem was designed under the assumption that enough fuel is carried to insure a probability of having sufficient fuel such that the over-all astrionics acceptable probability of failure is not exceeded. The acceptable probability of astrionics failure was specified as 0.15, the probability of failure due to lack of sufficient reliability was determined to be 0.09, and the probability of excessive target miss was essentially zero. This combination required the probability of having insufficient midcourse fuel to be 0.06. From the expected midcourse ΔV of 14.98 fps with 1 degree-of-freedom, the midcourse ΔV capability requirement, 28.15 fps, was then calculated. This resulted in a midcourse system weight, including nozzles, tankage, and fuel of 28.6 lb for mission schedule 1.

The weights of all the astrionics subsystems just discussed were totaled to obtain the effectiveness index or penalty of 343.46 lb for mission schedule 1. The total spacecraft was assumed to weigh 2000 lb. Thus, 1656.54 lb remain for structure and scientific payload.

A search for an optimum system operating on mission schedule 1 was conducted. The list of candidate components included four gyroscopes, four accelerometers, three computers, a strapdown or a gimballed star tracker, and a strapdown sun sensor. Only one communication receiver was in the list, so no optimization of this subsystem was performed. The evaluation considered the possibilities of not using electro-optical sensors. The optimum system was found to consist of GG177 accelerometers, 18 IRIG-B gyroscopes, a SIGN III computer, and the strapdown star tracker and sun sensor used in the reference system. The penalty for the optimum system is 331.45 lb compared to 343.46 lb for the reference system.

The reference and the optimum system found on mission schedule 1 were then evaluated using mission schedule 2. These results are shown in summary form in Table 2. The expected target miss distance for the optimum system is considerably larger than the expected miss distance of the reference system. However, since both distances are much less than the target miss requirement for the mission, this has negligible impact on the effectiveness index. The dominant factor is the actual physical hardware weight of the subsystem components.

An additional entry in Table 2 shows the results for the reference system evaluated on schedule 1 with the ground-based radar used for the range-rate measurement prior to the first midcourse degraded in accuracy. Increased update accuracies increase the required midcourse fuel and decrease target miss. If the target miss is already well below the mission requirement, P_{FT} remains essentially zero and hence only the increased penalty due to W_{DV} increase is noted. In actual operation, partial midcourse corrections rather than deliberate degradation of update accuracy would remove this effect.

Conclusions

An evaluation technique was developed for astrionics systems designed for interplanetary missions. This technique is useful for selection of astrionics subsystems, evaluating astrionics mission operation schedules, as an aid in the preliminary design of conceptual subsystems, and in determining research needed to improve system performance.

The system parameters used in the evaluation technique can be estimated using techniques that are relatively unsophisticated but are of sufficient accuracy to accomplish the desired result.

These techniques were implemented in computer programs now in use at NASA/ERC. The computer programs were exercised on a Jupiter flyby mission. Results indicate that present-day hardware, utilizing Kalman filtered updates, can provide the needed astrionics functions to accomplish a Jupiter flyby mission if the mission schedules are acceptable to spacecraft designers.

References

[1] Hitt, E. F. and Koenke, E. J., "An Evaluation Technique for Strapdown Guidance Systems on Interplanetary Missions," AIAA Paper 68-828, Pasadena, Calif., 1968; also *Journal of Spacecraft and Rockets*, Vol. 6, No. 5, May 1969, pp. 623–626.

[2] Hitt, E. F. and Rea, F. G., "Development of an Evaluation Technique for Strapdown Guidance Systems," Second Interim Scientific Report, Contract NAS 12-550, Feb. 28, 1969, Battelle Memorial Institute, Columbus Labs., Columbus, Ohio.

[3] Rea, F. G. and Fischer, N. H., "An Improved Method of Estimating Midcourse Fuel Requirements (Approximating the Probability Distribution of the Magnitude of a Vector with Normal, Zero Mean, Components)," Paper presented to NASA/ERC Fourth Guidance Theory and Trajectory Analysis Seminar, Cambridge, Mass., May 16–17, 1968.

[4] Strack, W. C. and Huff, V. N., "The N-Body Code, A General FORTRAN Code for the Numerical Solution of Space Mechanics Problems on an IBM 7090 Computer," TN D-1730, Nov. 1963, NASA.

[5] "Saturn IB Improvement Study (Solid First Stage) Phase II, Final Detailed Report," Rept. SM-51896, Vol. II, March 30, 1966, Douglas Missile and Space Systems Div., Huntington Beach, Calif.

[6] "Launch Vehicle Estimating Factors," Jan. 1969, NASA.

[7] "A Study of Jupiter Flyby Missions, Final Technical Report," FZM-4625, May 17, 1966, General Dynamics, Fort Worth Div., Fort Worth, Texas.

MARCH 1970 J. SPACECRAFT VOL. 7, NO. 3

Propellant Position Control by Capillary Barriers during Spacecraft Rotational Maneuvers

D. F. GLUCK*
North American Rockwell Inc., Downey, Calif.

Capillary barriers, which can provide a propellant positioning and expulsion capability for spacecraft propellant tankage, are used in some applications to create an engine restart compartment. However, pitch maneuvers cause propellant motions and inertial forces that act to draw gas through barrier perforations into the compartment. This is opposed by viscous stresses as well as capillary pressures developed by the barrier. From theory and experiments the dependence of the critical Weber number, We_c (Weber number at incipient gas passage through the barrier) during rotational maneuvers on geometry and fraction open barrier area, O_p, is given graphically. The effect of tank and barrier geometry on We_c is obtained by solving Laplace's equation based on an inviscid model of barrier gas-liquid interface dynamics for an impulsively rotated right cylinder. The effect on We_c of O_p, and thus viscous energy dissipation, was obtained from an experimental program of model tank rotations during aircraft Keplerian trajectories.

Nomenclature

a = tank radius
d = diameter of hole or perforation in capillary barrier
$F(t)$ = function of time in Bernoulli equation
g = acceleration or gravity field
h = height of the barrier above the tank bottom, where volume below barrier is taken as an equivalent right circular cylinder
J_1 = Bessel function of first order and first kind
l = normal distance from center of rotation to barrier
O_p = ratio of hole area to total barrier area
P = pressure; P_G = gas pressure
$\mathbf{q}$ = velocity vector
r = a cylindrical coordinate in inertial frame instantaneously coinciding with tank radial coordinate
R = radius of curvature
s = average height of liquid above capillary barrier
t = time
U = velocity in x direction
V = volume of spherical segment
W = velocity in Z direction
We_c = critical Weber number, value of Weber number at incipient gas passage through barrier
W_R = velocity of liquid through barrier hole relative to tank velocity
$\langle W \rangle_R$ = average value of W_R during growth of interface to maximum size
W_t = tank velocity in Z direction
x = coordinate in inertial framework
X = height of spherical segment
Z = coordinate in inertial frame instantaneously coinciding with the tank axis, taken as positive in the downward direction
η = coefficient of bubble pressure term
$\dot{\theta}$ = rotation rate about axis perpendicular to tank longitudinal axis
ν = kinematic viscosity
ξ_n = roots of J_1 (arg) = 0
ρ = liquid density
σ = liquid surface tension
φ = angular coordinate in inertial framework instantaneously coinciding with tank coordinate
Φ = velocity potential
Φ_F = final velocity potential for case of O_p approaching 1
Φ_0 = initial velocity potential for case of O_p approaching 1

Presented as Paper 69-529 at the AIAA 5th Propulsion Joint Specialist Conference, U.S. Air Force Academy, Colo., June 9–13, 1969; submitted June 9, 1969; revision received October 27, 1969.

* Member of the Technical Staff.

Introduction

CAPILLARY barrier devices can provide a propellant positioning and expulsion capability, as well as appreciable slosh dampening, for spacecraft propulsion systems. Such devices, which are sometimes simply perforated plates, function both by utilizing propellant surface tension to generate motion-inhibiting capillary pressures and by providing a mechanism for viscous energy dissipation. The configuration studied herein is one which might be used in a restartable propulsion system that experiences periods of near weightlessness alternating with periods of propellant orienting engine thrust. Referring to Fig. 1, it is obviously important